

Abstract: Ocean currents can strongly impact the propagation of swell systems. Satellite altimetry routinely provides measurements of ocean surface significant wave heights (Hs). A self-consistent space-scale decomposition is applied to Hs measurements obtained from different altimeters. This method helps reveal overlooked statistical properties at scales less than 100 km, where meso- and submesoscale upper ocean circulation traces a significant part of the variability in the coupled ocean-atmosphere system. In particular, systematic signatures related to wave-current interactions are well evidenced at global and regional scales. In the Agulhas current system, the proposed space-scale decomposition further reveals organized and persistent patterns. In leading order, the redistribution of swell energy follows the cumulative impact of the large-scale current vorticity field on wave train kinematics. This relationship causes significant swell-ray deflection and localized trapping phenomena, which are adequately captured by altimeter measurements.

Denoising of along-track altimeter 1 Hz data with Empirical Mode Decomposition (EMD)

The main sources of noise and errors come from the altimeter waveform retracking algorithms, instrumental noise, and geophysical variability within the altimeter footprint. Analysis of fine scale ocean dynamics then requires preliminary signal filtering and low-pass or smoothing filters are frequently used. This filtering operation results in loss of small scale geophysical information and may also create artifacts in the spectral content of the analyzed variability. We use a different approach whose key part is the Empirical Mode Decomposition. EMD is a method to decompose signals into a finite and often small number of AM-FM components, called intrinsic mode functions (IMF). Because the decomposition is based on the local characteristic sampling scale of the data, it is applicable to nonlinear and nonstationary processes. The EMD method ranks, by construction, the IMFs from the one containing the smallest scales (mainly noise) to the last one containing the overall trend. The noise filtering rules rely on the property that ADT acts as a dyadic filter bank in case of a signal containing pure gaussian noise, featuring a well defined linear decrease of noise variance with increasing IMF rank. EMD is particularly relevant because our data set combines measurements from different sensors with different noise characteristics. As shown in Figure 1, the variance in the first SSH IMF strongly reflects the noise characteristics. The Figure 2 shows the power spectral density for the noisy and denoised measurements of absolute dynamic topography and significant wave height.

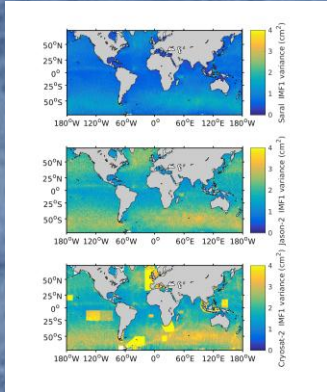


Figure 1. Variance in the first intrinsic mode function (IMF1) derived from raw 1 Hz measurements from SARAL/AltiKa (top panel), Jason-2 (middle panel), and Cryosat-2 (bottom panel) on a 1° x 1° grid.

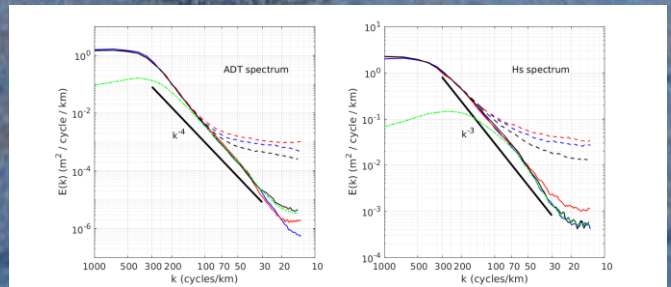


Figure 2. Power spectral density as a function of wavenumber (x-axis labels in km) for altimeter measurements of absolute dynamic topography (left) and significant wave height (right): SARAL/AltiKa (black), Cryosat-2 (red) and Jason-2 (blue), time period 2014 - 2016. Agulhas region. Dashed (solid) lines are for raw (filtered) 1 Hz data. The first intrinsic mode function (IMF) PSD of filtered ADT (left) and Hs (right) is shown as a dashed-dotted green line. Solid black lines give the k^{-4} (left) and k^{-3} (right) dependence between 300 km and 30 km of wavelength.

Persistent small scale signatures of waves / current interactions

As discussed in the previous section, the EMD-based methodology self-adjusts to the different altimeter instruments to best remove the noise. A second EMD analysis is further performed on the denoised data. The resulting first IMF shall then solely contain information related to the geophysical small mesoscale variability down to the altimeter sampling capability. The higher-order IMFs will carry information related to very large-scale variability and trends. The spatial distribution of the first IMF variance is shown in Figure 3. For the Agulhas region, the corresponding spectral content is shown in Figure 1 as green dashed-dotted lines. The effectiveness of the EMD denoising approach is illustrated by comparing the first IMF patterns obtained from the raw ADT data set (Figure 1) with those obtained from the filtered data (Figure 3, top). The ADT variance patterns obtained from the filtered data are closely related to the expected location of the main dynamical and/or rich-eddy regions. The global map of the Hs variance demonstrates large mesoscale variability that almost coincides with the ADT variance patterns. This finding provides striking evidence of global wave/current interactions that shape global sea state variability.

To explain such co-variation analysis, the figure 4 illustrates the trajectories followed by a given storm swell coming from the southern latitudes and entering in the Agulhas current system. The wave spectrum evolution in presence of currents depends mainly on the refraction of waves (function of the ratio current vorticity / wave group velocity) and from the advection of wave action by the current vector. As shown, rays converge in areas called “caustics”, where increased sea states are found as a result of conservation of wave action. Opposite, lower sea state are found in other areas (see Quilfen et al., RSE 2018).

More statistical results are presented in Figure 6. The Agulhas region is an avenue for swells generated in southern latitudes by storms (see Figure 5, top, showing the peak wave direction at the southwestern boundaries of the area displayed Figure 4). The wave conditions presented in the case study of Figure 4 prevail in this area. Mean Hs anomalies in the Agulhas region from 2014 – 2016 are shown in Figure 6, top, and the mean density of rays is shown in the bottom panel. For each day, the daily CMEMIS current field has been used to predict the ray field. Persistent patterns clearly result from the cumulative impacts of the large-scale and persistent nature of the current vorticity field on wave train kinematics. Because of the significant ray deflection and trapping phenomena, localized sea state gradients can be anticipated and are well traced in altimeter signals.

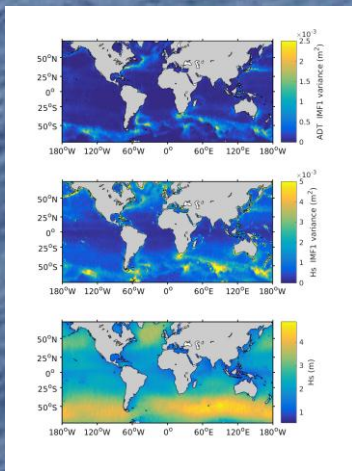


Figure 3. Mean field of the first intrinsic mode function of denoised ADT (top) and Hs (middle) data and the corresponding mean total Hs field (bottom). Mean estimates are computed on a 1° x 1° lon/lat grid using data from the 3 altimeters, 2014 - 2016.

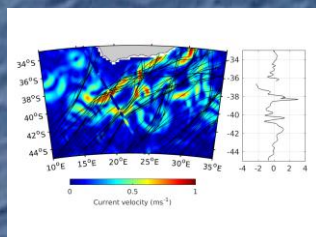


Figure 4. Surface current velocity on February 28th, 2016, and superimposed swell rays (solid black lines). Jason-2 Hs anomalies (cycle 282, pass 46) are shown on the left panel (color-coded) and the right panel. All Hs anomalies are denoised Hs values computed as the sum of IMFs for the analyzed data segment, except the last IMF, which represents the trend.

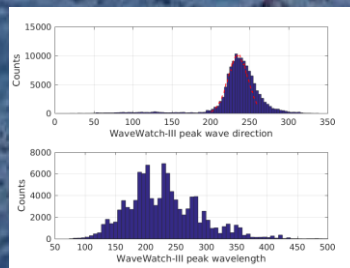


Figure 5. Distribution of the WaveWatch-III spectrum peak direction (top, in degrees clockwise / north) and wavelength (bottom,). The dashed red line shows the truncated gaussian distribution used for rays simulation.

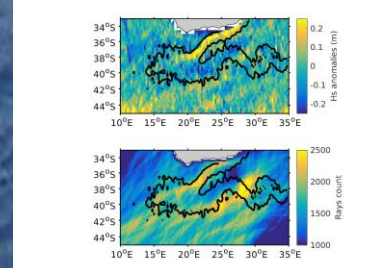


Figure 6. Mean values (2014-2016) in a 0.25° x 0.25° grid of Hs anomalies (top) and mean number of swell rays (bottom). Rays are generated for a random Gaussian distribution of swells coming from the southwest corner of the area with a given wavelength of 250 m and varying directions with a mean and standard deviation of 52° (clockwise relative to north) and 13°, respectively. The solid black line indicates the 0.5 m/s isocontour of mean surface current velocity.